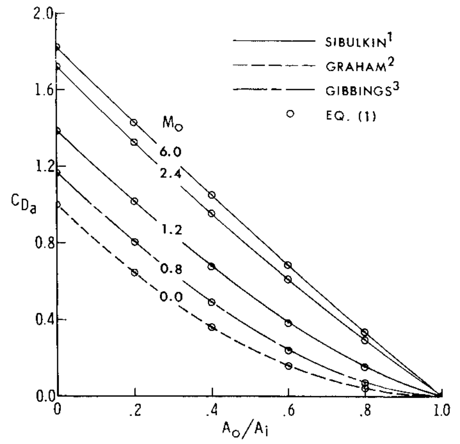

Fig. 3 Comparison of C_{Da} by present method and other analytical sources.

$$C_{D_a} = C_{P_s}(1 - A_0/A_i) \quad \text{at} \quad A_0/A_i = 1.0 \qquad (8)$$

$$dC_{D_a}/d(A_0/A_i) = -2 \quad \text{at} \quad A_0/A_i = 0 \qquad (9)$$

$$dC_{D_a}/d(A_0/A_i) = -C_{P_s} \quad \text{at} \quad A_0/A_i = 1.0 \qquad (10)$$

Equation (6) is identical to the incompressible form of C_{D_a} derived by Graham.[2] Equation (7) concurs with Sibulkin's[1] derivation when his equation is evaluated at zero capture area ratio. The properties defined by Eqs. (8–10), however, are not readily deducible from Sibulkin although curves based on his equations appear to be compatible in trend. In Fig. 3, values of C_{D_a} from Eqs. (1–5) are compared with analytical levels presented by Sibulkin and others.[3,4] The agreement is generally well within ± 0.003.

Experimental data presented in Refs. 1 and 5 substantiate theory at M_0 values of 1.42–1.87. Figure 4 presents further substantiating data[6] acquired at the General Dynamics/Convair High Speed Tunnel during tests with a series of sharp-lip and blunt-lip cowls. Additive drag was determined by means of pressure rake instrumentation at the inlet, metered duct flow, and application of flow continuity considerations. The results at M_0 values of 1.80, 1.20, and 0.86 are typical and agree well with C_{D_a} from Eq. (1).

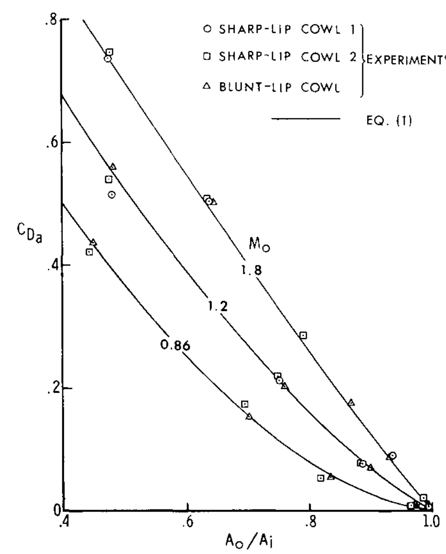

Fig. 4 Comparison of C_{Da} by present method and experimental measurement.

References

[1] Sibulkin, M., "Theoretical and Experimental Investigation of Additive Drag," Rept. 1187, 1954, NACA.

[2] Graham, E. W., "Notes on the Drag of Scoops and Blunt Bodies," Rept. SM-13747, April 1950, Douglas Aircraft Co.

[3] Gibbings, J. C., "Pressure Measurements on Three Open Nose Air Intakes at Transonic and Supersonic Speeds, with an Analysis of Their Drag Characteristics," C.P. 544, 1961, Aeronautical Research Council.

[4] Seddon, J., "Note on the Spillage Drag of Pitot-Type Air Intakes at Transonic Speeds," TN Aero 2315, Aug. 1954, Royal Aircraft Establishment.

[5] Griggs, C. F. and Goldsmith, E. L., "Measurements of Spillage Drag on a Pitot-Type Intake at Supersonic Speeds," TN Aero 2256, Aug. 1953, Royal Aircraft Establishment.

[6] "Research Summary, Applied Research Program, July–December 1965," ARR-9, April 1966, General Dynamics, Fort Worth, Texas.

Solutions for Axially Symmetric Orthotropic Annular Plates

R. H. Bryant*
University of Illinois, Chicago, Ill.

Nomenclature

A,B,C,E	=	arbitrary constants
a	=	radius of plate
D_r,D_θ	=	plate constants in the radial and circumferential directions
k	=	$(D_r/D_\theta)^{1/2}$
M	=	bending moment
M_r,M_θ	=	radial bending moment and circumferential bending moment
P	=	point load
Q_r	=	transverse shearing force
q,q_0	=	lateral loading
r	=	radial coordinate
r_0,r_1	=	coordinate for starting function
w	=	lateral deflection
w_d,w_r,w_m w_Q,w_l	=	starting functions for unit deflection, unit slope, unit moment, unit shear, and unit lateral load, respectively
w_p	=	particular solution
$\alpha_{ij}(r)$	=	slope, or stress field for various starting functions as noted in Table 2
ν_r,ν_θ	=	Poissons ratio in radial and circumferential direction

Introduction

A SYSTEM of starting functions for solving annular orthotropic plate problems are presented. At a given radial coordinate, r_0, r_1, etc., a particular function will give a unit intensity for one field quantity and zero for all others. The technique of generating solutions to problems is indicated with an example.

Formulation of Starting Functions

The equilibrium equation for axisymmetric problems for classical plate theory is given by Eq. (1)

$$w'''' + (2/r)w''' + k^2[-(1/r^2)w'' + (1/r^3)w'] = q(r)/D_r \qquad (1)$$

Table 1 Starting functions and stresses

w	(dw/dr)	M_r	M_θ	Q_r	q
w_d	0	0	0	0	0
w_r	α_{21}	α_{22}	α_{23}	0	0
w_m	α_{31}	α_{32}	α_{33}	0	0
w_Q	α_{41}	α_{42}	α_{43}	α_{44}	0
w_l	α_{51}	α_{52}	α_{53}	α_{54}	α_{55}

Received March 31, 1970.

* Assistant Professor of Structural Mechanics, Department of Materials Engineering.

Table 2 List of functions defined in Table 1

$$w_d = 1$$

$$w_r = -[r_0/2k(1 - k^2)][2k(1 + \nu_\theta) - (1 - k)(k - \nu_\theta)(r/r_0)^{1+k} - (1 + k)(k + \nu_\theta)(r/r_0)^{1-k}]$$

$$w_m = -[r_0^2/2k(1 - k^2)D_r][2k + (1 - k)(r/r_0)^{1+k} + (1 + k)(r/r_0)^{1-k}]$$

$$w_Q = r_0^3/2k(1 - k^2)D_r\ [k - k(r/r_0)^2 + (r/r_0)^{1+k} - (r/r_0)^{1-k}]$$

$$w_l = [r_0^4/8k(1 - k^2)(9 - k^2)D_r][k(9 - k^2) - 2k(9 - k^2)(r/r_0)^2 + 4(3 + k)(r/r_0)^{1+k} - 4(3 - k)(r/r_0)^{1-k} + k(1 - k)(r/r_0)^4]$$

$$\alpha_{21} = 1/2k[(k - \nu_\theta)(r/r_0)^k + (k + \nu_\theta)(r/r_0)^{-k}]$$

$$\alpha_{22} = [(k - \nu_\theta)(k + \nu_\theta)/2kr_0][(r/r_0)^{-k-1} - (r/r_0)^{k-1}]$$

$$\alpha_{23} = -D_\theta/2kr_0[(k - \nu_\theta)(k\nu_\theta + 1)(r/r_0)^{k-1} + (k + \nu_\theta)(1 - k\nu_r)(r/r_0)^{-k-1}]$$

$$\alpha_{31} = -(r_0/2kD_r)[(r/r_0) - (r/r_0)^{-k}]$$

$$\alpha_{32} = -1/2k[(k + \nu_\theta)(r/r_0)^{k-1} + (k - \nu_\theta)(r/r_0)^{-k-1}]$$

$$\alpha_{33} = -k/2[(k\nu_r + 1)(r/r_0)^{k-1} + (k\nu_r - 1)(r/r_0)^{-k-1}]$$

$$\alpha_{41} = -r_0^2/2k(1 - k^2)D_r[2k(r/r_0) - (1 + k)(r/r_0)^k + (1 - k)(r/r_0)^{-k}]$$

$$\alpha_{42} = r_0/2k(1 - k^2)[2k(1 + \nu_\theta) - (1 + k)(k + \nu_\theta)(r/r_0)^{k-1} - (1 - k)(k - \nu_\theta)(r/r_0)^{-k-1}]$$

$$\alpha_{43} = kr_0/2(1 - k^2)[2k(1 + \nu_r) - (1 + k)(1 + k\nu_r)(r/r_0)^{k-1} + (1 - k)(1 - k\nu_\theta)(r/r_0)^{-k-1}]$$

$$\alpha_{44} = r_0/r$$

$$\alpha_{51} = r_0/2k(1 - k^2)(9 - k^2)D_r[k(9 - k^2)(r/r_0) + (1 - k)(3 + k)(r/r_0)^k - (1 - k)(3 - k)(r/r_0)^{-k} + k(1 - k^2)(r/r_0)^3]$$

$$\alpha_{52} = -(1 + \nu_\theta)/2(1 - k^2) - r_0^2/2k(1 - k^2)(9 - k^2)[(1 + k)(3 + k)(k + \nu_\theta)(r/r_0)^{k-1} + (1 - k)(3 - k)(k - \nu_\theta)(r/r_0)^{-k-1} + k(1 - k)(3 + \nu_\theta)(r/r_0)^2]$$

$$\alpha_{53} = -k^2(\nu_r + 1)/2(1 - k^2) - [kr_0^2/2(1 - k^2)(9 - k^2)][(1 + k)(3 + k)(1 + k\nu_r)(r/r_0)^{k-1} + (1 - k)(3 - k)(k\nu_r - 1)(r/r_0)^{-k-1} + k(1 - k)(1 + 3\nu_r)(r/r_0)^2]$$

$$\alpha_{54} = (r_0^2/2r) - (r/2)$$

$$\alpha_{55} = 1$$

The solution of Eq. (1) may be obtained by direct integration and is given by

$$w = A + Br^2 + Cr^{1+k} + Er^{1-k} + w_p \qquad (2)$$

The stress resultants are given by

$$M_r = -D_r[w'' + (\nu_\theta/r)w'],\ M_\theta = -D_\theta[\nu_r w'' + (1/r)w']$$
$$Q_r = -D_r[w''' + (1/r)w''] + D_\theta(1/r^2) \qquad (3)$$

The quantities in Eqs. (1–3) are defined in the nomenclature.

In the solution of annular plate problems if Eq. (2) is used directly, it becomes necessary to satisfy the boundary conditions at the inner and outer edges of the plate and to satisfy the continuity conditions on deflection, slope, bending moment, and shear force for a discontinuity in the loading function. It is possible to choose a linear combination of the functions given by Eq. (2) such that at a given radial coordinate all the resultant field equations are zero except for one. Likewise, it is possible to choose a w_p such that all field quantities are zero at a particular coordinate. Hence, it is possible to start or alter a solution by choosing the correct starting function for a plate, one of the derived starting functions will yield the solution within an arbitrary constant.

Table 3 Starting functions for different boundary conditions

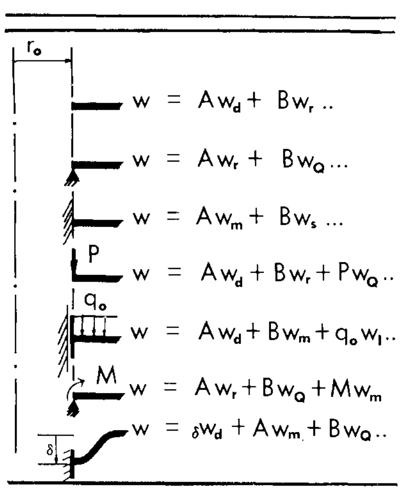

The derivation of the starting functions is straightforward and only the results will be presented here. It is enough to note that at $r = r_0$ ($r = r_1$, etc.) w_d gives a unit deflection and zero fields, w_r gives a unit slope and zero fields, similarly w_m gives a radial moment intensity, w_Q a unit shearing force intensity, and w_l satisfies the equilibrium equation for a lateral load of unit intensity. All the functions and their resultant field quantities are tabulated in Table 1. Table 2 expresses the functions explicitly. Table 3 indicates how the functions may be used to start a problem for some given boundary conditions at r_0.

To indicate the use of the tables consider the plate shown in Fig. 1. The plate has a rigid inner core of radius r_0, lateral loads P and q, and is simply supported at the outer boundary

$$\text{for } r_0 \leq r \leq r_1,\ w_1 = Aw_d + Bw_m + (P/2\pi r_0)w_Q$$
$$\text{for } r_1 < r \leq a,\ w = w_1 + q_0 w_l \qquad (4)$$

The boundary conditions, $w = 0$ and $M_r = 0$ at $r = a$ yields

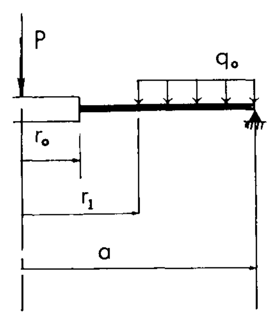

Fig. 1 Simply supported annular plate with rigid boss.

the following equations for A and B,

$$B = [(P/2\pi r_0)\alpha_{x2}(a) + q_0\alpha_{52}(a)]/\alpha_{32}(a)$$
$$A = [(P/2\pi r_0)\alpha_{42}(a) + q_0\alpha_{52}(a)]^{w_m(a)}/\alpha_{32}(a) \quad (5)$$
$$(P/2\pi r_0)w_Q(a) - q_0 w_l(a)$$

provided $k \neq 1$.

The expressions in Eq. (5) may now be obtained by direct substitution from Table 2. The procedure is straightforward and the example, will not be persued further.

Summary

Starting functions for the solution of axisymmetric orthotropic annular plates are given along with their stress resultants. An example indicating their use was presented. It was shown that the arbitrary constants used in starting the problem could be obtained from the outer boundary condition. It should be pointed out that w_l may also be used for the case of variable loading. A similar set of starting functions may also be devised for other problems, for example, thick plates.

Reference

[1] Lekhnitskii, S. G., *Anisotropic Plates*, 2nd ed., Gordon and Breach, New York, 1968, p. 370.

Upwash Interference on a Jet Flap in Slotted Tunnels

Ching-Fang Lo*
ARO Inc., Arnold Air Force Base, Tenn.

Introduction

THE V/STOL models used in the development of a wind-tunnel wall configuration for V/STOL testing should include a spectrum of models from the high disk loading (e.g., lifting jet, lifting fan, and rotor) to the low disk loading models (e.g., jet-flat wing). The high disk loading model in slotted-wall tunnels has been investigated by the author in Refs. 1–3. The interference of a jet-flap wing in slotted-wall tunnels will be considered as part of the program in the present study. A detailed mathematical treatment of this problem has not yet become available,[4] although some qualitative discussions are presented in Ref. 4 for the closed-wall tunnel.

This paper presents the upwash interference on a two-dimensional jet-flap wing in a slotted-wall tunnel. The formulation is based on the small disturbance theory and the linearized model of the jet-flap wing as derived by Spence.[5] An analytical solution is developed for the upwash interference and some numerical results are shown in the graphical form.

Analysis

The field equation of an inviscid, irrotational fluid for incompressible flow in terms of the perturbation velocity potential φ in Cartesian coordinates (Fig. 1) is

$$[(\partial^2/\partial X^2) + (\partial^2/\partial Y^2)]\varphi = 0 \quad (1)$$

The boundary conditions for the slotted walls using an equivalent homogeneous boundary condition[1] are expressed as

$$\varphi \pm (K\partial\varphi/\partial Y) = 0,\ Y = \pm H \quad (2)$$

where K is related to the wall porosity a/l as $K = (l/\pi)\ln[\csc(\pi a/2l)]$. The slot parameter is introduced as $P = (1 + K/H)^{-1}$ where the value of $P = 0$ corresponds to a closed wall and $P = 1$ to an open wall. Note that the geometric slot constant, K, in Eq. (2) may also be related to the wall porosity a/l by $K = [(l - a)/2]\tan[\pi(1 - a/l)/2]$ as in Ref. 8. This gives a good correlation between theory and experiment in some slotted wind tunnel investigations.

The linearity of the field equation and its boundary condition permits the perturbation potential to be separated into two parts as $\varphi = \varphi_m + \varphi_i$ where φ_m is the disturbance potential caused by the model in free air and φ_i is the interference potential induced by the tunnel walls.

The two-dimensional jet-flap wing located at the centerline in a slotted-wall wind tunnel is shown in Fig. 1a. The linearized model of a jet-flap wing shown in Fig. 1b has been analyzed by the small disturbance theory.[5] The airfoil and jet are represented by the vorticity distribution γ which

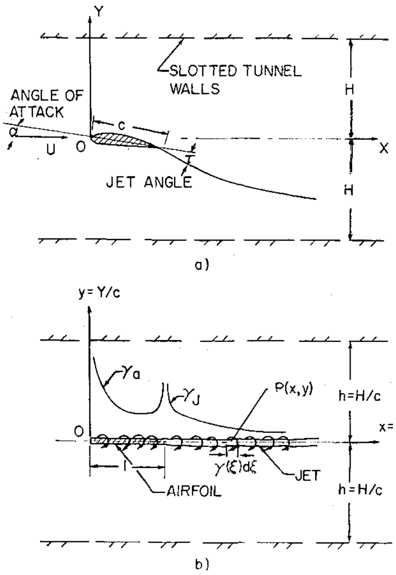

Fig. 1 Jet-flap wing in a slotted-wall wind tunnel and its mathematical model.

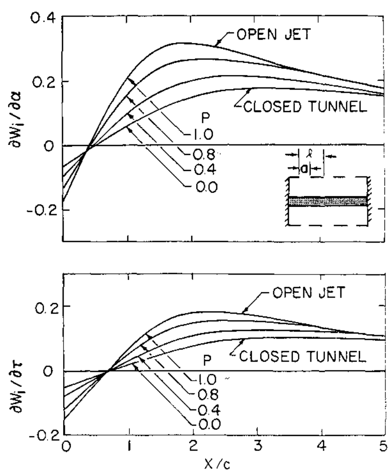

Fig. 2 Upwash interference for a jet-flap wing with C_J = 2.0 in a slotted tunnel with various wall porosities at H/c = 1.5.

Received June 19, 1970. The research reported herein was sponsored by the Arnold Engineering Development Center, Air Force Systems Command, under Contract F40600-69-0001 S/A 10(70) with ARO Inc. Further reproduction is authorized to satisfy needs of the U.S. Government.

* Research Engineer, Propulsion Wind Tunnel Facility. Member AIAA.